

NORMAL TEMPERATURE AND ICE COVER OF THE GREAT LAKES*

K. Schneider
Institut für Geographie, Universität München
80333 München, Germany

Assel R.A and T.E. Croley II
NOAA/GLERL
Ann Arbor, MI, U.S.A.

ABSTRACT

A long-term average (normal) temperature and ice cover data base was created together with a computer program to display and analyze different aspects of temperature and ice cover in the Great Lakes. The daily normal surface temperature of each of the Great Lakes was derived from remotely-sensed data acquired between 1966 and 1993. Normal ice cover maps, from the NOAA Great Lakes Ice Atlas, were interpolated to yield daily patterns and converted to a Mercator projection with a 2.5 km grid resolution. Two-dimensional surface temperature and ice data, bathymetry maps, and normal daily vertical temperature profiles were combined into a database for an analysis and animation program. This interactive, menu-driven computer program has four main modules: a) two-dimensional normal daily surface temperature and ice patterns, b) horizontal surface temperature profiles, c) normal daily vertical temperature depth profiles and d) surface temperature and ice cover versus bathymetry.

1.0 INTRODUCTION

Lake surface temperature is a critical factor for many physical, biological, and chemical studies. It is an integrated expression of past meteorology, heat storage, and lake dynamics. Lake surface temperatures and ice cover show horizontal patterns, which result from the complex interaction of energy fluxes, heat storage, and limnokinetics. Due to their large energy storage capability, lakes integrate energy fluxes over long time periods and are therefore especially sensitive to changes in the magnitude and temporal course of energy fluxes which occur as a result of changing climatic conditions.

The horizontal structure of ice cover and surface temperature has been published earlier as printed maps. Based on remote sensing data, a 20-winter average (normal) of the spatial and seasonal pattern of ice cover concentration for the Great Lakes was published from ice charts produced during the 1960s and 1970s (Assel et al., 1983). More recently, a 23-year (1966-1988) Great Lakes surface water temperature climatology was published (Irbe, 1992). These two publications contain maps which provide very useful information about ice cover and lake surface temperature seasonal and spatial patterns.

To provide a more complete view of the long-term thermal characteristics of the Great Lakes, we produced a combined normal surface temperature and ice cover data base, and included modelled mean lakewide vertical temperature profiles to display the relationship between surface temperature and ice cover and heat storage. Understanding the spatial and temporal dynamics of temperature and ice cover patterns is very difficult from time series of climatological maps. Furthermore, paper charts do not convey easy data access for further research. Computer data bases coupled with a visualization and analysis program can solve these shortcomings

*Presented at the Second Thematic Conference on Remote Sensing for Marine and Coastal Environments, New Orleans, Louisiana, USA, 31 January - 2 February 1994

of printed maps and improve the understanding of lake dynamics (Leshkevich, 1982; Assel and Ratkos, 1991).

We developed a computer program to display and analyze various aspects of Great Lakes temperature and ice cover patterns. The interactive, menu-driven computer program was written for an IBM-compatible PC running under DOS, with a color VGA graphics adapter. It displays two-dimensional patterns of temperature and ice cover in animated sequences. The dependence of temperature and ice cover patterns on the depth of the lake can be investigated by direct comparison of two-dimensional temperature and ice cover patterns with the lake bathymetry or by plotting temperature and ice cover versus bathymetry. Horizontal temperature profiles along user-defined trajectories can be selected and presented in line drawings. Normal temperature profiles for each Great Lake are presented to study the dependency of surface temperature and ice cover patterns on temperature and heat storage of the underlying water column. The data bases for normal surface temperature and ice cover and vertical temperature profiles are fully documented and build, along with bathymetric data, a data base for a variety of further research.

2.0 DATA SOURCES, PROCESSING, ANALYSIS

The two dimensional temperature and ice cover data bases were compiled by using data from different sources. These are: air-borne and satellite-borne surface temperature data, visual aerial ice reconnaissance overflights and side looking airborne radar (SLAR) data to produce ice charts, and gridded bathymetry data published by Schwab and Sellers (1980).

For each lake, a normal temperature data base, a normal ice cover data base and a bathymetry data base were generated separately. Ice cover, surface water temperature and lake bathymetry data were mapped to a common grid with a 2.5 km grid resolution in a Mercator projection. Subsequently these data bases were combined to yield a normal temperature and ice cover data base for each Great Lake. The generation of the normal ice cover data base, the normal temperature data base, and the bathymetry data base and the combination technique for these data bases is discussed in more detail in the following paragraphs.

2.1 ICE COVER DATA

More than 2800 digitized ice charts acquired between 1960 and 1979 were used to generate normal ice charts for each Great Lake (Table 1). The original ice charts were heterogenous in spatial and temporal coverage,

Table 1. The GLERL Ice Cover Data Base

Lake	-----Number of-----		Total number of observations
	Ice Charts	Grid Cells	
Superior	618	3,195	1,974,510
Michigan	489	2,224	1,087,536
Huron	845	2,308	1,950,260
St.Clair-Erie	565	1,041	588,165
Ontario	307	739	226,873
Total	2,824	9,507	5,872,344

making it untenable to perform analysis below a half month time period. Thus, the gridded data were divided into nine half-monthly periods (HMP), starting 16-31 December and ending 16-31 April. For each HMP the normal ice concentration was defined as the median (instead of mode or average) ice concentration (Assel et al., 1983), because it provided the most coherent spatial and season pattern of ice formation and loss. Daily ice concentration maps were derived by linear interpolation between each grid cell of each of the nine HMP normal (median) ice charts given in the *NOAA Great Lakes Ice Atlas* for each Great Lake. This resulted in 121 normal daily ice charts for each Great Lake starting 22 December, the midpoint of the first HMP and ending 22 April, the midpoint of the ninth HMP. These normal daily ice charts represent the transition from the normal ice concentration distribution patterns of one HMP to the normal ice concentration distribution patterns of the next HMP. Thus the normal daily ice charts are not a true daily normal for any given date, but they nevertheless are useful in illustrating the spatial and temporal change in the normal ice cover given in the *NOAA Great Lakes Ice Atlas*. The interpolated ice concentrations were rounded to the nearest 10% increment; for example, 12% ice concentration was recorded as 10%, and 16% was recorded as 20%. This rounding was done to be consistent with the accuracy of the original data. A detailed description of the interpolation procedure and methodology is available elsewhere (Assel and Ratkos, 1991).

2.2 LAKE SURFACE TEMPERATURE DATA

The "normal" annual cycle of the water surface temperature is based on data acquired by the Canadian Atmospheric Environment Service (AES) and by NOAA's Great Lakes Environmental Research Laboratory (GLERL) from 1966 to 1993. Table 2 shows the total number of images available to this study. Since the number of images acquired by GLERL for all lakes exceeds the number of images available through AES, the normal surface temperature is biased by the higher abundance of images since 1990. However, comparing the normal temperature patterns displayed here with the climatological temperature patterns published in the *Great Lakes Surface Water Climatology* (Irbe, 1992) reveals the same major temperature patterns, and thus the bias can be considered small.

Table 2. Number of images for normal temperature calculation

Lake	Period	AES		Period	GLERL		Total Images
		Images	Gridpts		Images	Gridpts	
Superior	1966-1990	236	150	1990-1993	536	12970	772
Michigan	1966-1990	77	164	1990-1993	627	8031	704
Huron	1966-1990	327	188	1990-1993	553	8234	880
St.Clair	1966-1990	0	0	1990-1993	544	126	572
Erie	1966-1990	417	81	1990-1993	544	3292	961
Ontario	1966-1990	509	64	1990-1993	565	2514	1074

Due to energy losses from longwave radiation, convection and evaporation, which occur within the uppermost millimeter of the water column, remotely measured surface skin temperatures are usually some tenths of a degree Celsius cooler than the temperature of the directly underlying, well-mixed water layer (Ewing and McAlister, 1960; McAlister and McLeish, 1969; Paulson and Parker, 1972; Grassl, 1976; Schneider and Mauser, 1991; Schneider, 1992).

Remote sensing temperature measurements are limited to cloud-free atmospheric conditions. A fractional cloud

cover covering only 1% of a pixel can lead to a temperature error of 0.2 °C or more (Saunders, 1986). Thus a major processing step to derive surface temperatures from remote measurements is the detection and elimination of clouds.

Even a cloud-free atmosphere affects radiative surface temperature measurements, because the atmosphere absorbs radiation emitted by a lake surface and emits thermal radiation according to its own temperature and emissivity (Schneider et al., 1990). The atmospheric effect on remote temperature measurements is largely dependent on the water vapor content in the atmosphere (Bernstein, 1982) and usually reduces the satellite-measured absolute temperature and decreases the temperature range. The atmospheric effect is corrected by applying a split window correction algorithm which uses the wavelength dependency of the radiation absorbed by the atmosphere, or by modeling the atmospheric attenuation with an atmospheric radiation and transmittance model (McClain et al., 1985; Byrnes and Schott, 1986; Wilson and Anderson, 1986; Walton, 1988; Schneider, 1992)

Due to their different origin and processing levels, the AES and GLERL surface temperature data sets were processed differently and then combined.

The AES dataset consists of airborne and satellite-borne radiometric surface temperature measurements. Airborne surface temperature measurements were taken between 1966 and 1979. Starting in 1980, surface temperature maps were derived from satellite images of the NOAA Advanced Very High Resolution Radiometer (AVHRR). Lake Michigan surface temperature maps have been processed since 1987. Black Bay and Nipigon Bay in Lake Superior, Lake St. Clair, and North Channel were not represented in the AES grid. The dataset provided by AES is sampled to a grid with a 5 minute latitude/15 longitude spacing and tailored to suit the size and shape of each lake (Irbe, 1992).

AES surface temperature data are atmospherically and geometrically corrected. A comparison of 452 satellite-based temperature measurements with buoy measurements at 1-m depth yielded an average difference of 0.3°C, and a standard deviation of 0.9°C. Fifty-one intercomparisons for airborne measurements with submerged thermistors and ship buckets revealed a 0°C average difference and a standard deviation of 0.6°C (Irbe, 1992). Given that radiometric temperature measurements take place within the viscous boundary layer and that conventional measurements are taken within the turbulent mixed zone below this boundary layer, this difference is negligible from a climatological viewpoint.

To combine the AES surface temperature measurements with GLERL satellite images, we extrapolated the surface temperatures for each observed day with more than 33% observed grid points to the 2.56-km grid by using an inverse squared-distance weighting method.

Since 1990, GLERL has received satellite images from NOAA satellites on an operational basis (Leshkevich et al., 1993) in its CoastWatch program. The data are calibrated, quality controlled, earth located, and atmospherically corrected by NOAA's National Environmental Satellite, Data, and Information Service (NESDIS), mapped to a Mercator projection, and resampled to a 512x512 pixel grid (Maturi and Taggart, 1993). To be compatible with this dataset, the grid used to process the normal surface temperature and ice cover was adapted from the full region, Mercator projection grid of the CoastWatch dataset. The grid spacing is 2.56 km at mid latitude.

GLERL surface temperature data are based solely on images from the NOAA/AVHRR. Only fully atmospheric corrected images of AVHRR-11 were used in this study. AVHRR-11 is equipped with three spectral bands in the thermal infrared region, and therefore enables correction of atmospheric attenuation using a multiple window algorithm. These multichannel equations are based on the observation that atmospheric attenuation depends on wavelength, whereas atmospheric radiation is largely independent of wavelength (Viehoff, 1983). Therefore the

atmospheric effect can be calculated from two or more independent spectral measurements in the thermal infrared.

The majority of the GLERL temperature images used in this study yielded a mean difference between buoy measurements at 0.5 m depth and AVHRR temperatures of -0.11°C for daytime images and -0.03°C for nighttime images. A different atmospheric correction algorithm used during the first phase of the Coastwatch program resulted in mean differences of 1.13°C for daytime images and 1.72°C for nighttime images (Leshkevich et al., 1993).

The data received by GLERL have not been tested for cloud contamination. To extract meaningful lake surface temperature data from these satellite measurements, the data are tested for cloud cover and cloud contamination in a four-step automatic cloud-testing procedure. Cloud-free lake surface temperature for each lake is extracted from the original satellite images and used in further image processing steps if at least 33% of the lake surface tested cloud free. Small cloud-contaminated areas are filled by using an inverse squared-distance weighting method and by averaging cloud-free pixels within seven pixels from the cloud-contaminated grid point. The results of these automatic processing steps are visually checked and corrections are performed manually.

2.3 PROCESSING NORMAL TEMPERATURE PATTERNS

The total number of images used to calculate the normal surface temperature pattern is shown in Table 2. Since AVHRR data are available to GLERL on an operational basis, the frequency of surface temperature images has increased considerably since 1990. Due to spatially and temporally changing cloud cover, the surface temperature dataset is not homogeneous. The typical long-term temperature, defined here as normal temperature, of each grid point and day of the year cannot be calculated as the arithmetic mean over all such days of all years, since each grid point and day has a different observational base. Especially in the late fall and winter, the high probability of cloud cover decreases the frequency of satellite-derived surface temperature images considerably.

Following a method described by Irbe (1992), the normal lake surface temperature was derived using a regression method. A day number was assigned to each image according to its day of the year (Julian day). A linear least squares regression of temperature and Julian day number was calculated on segments of the dataset. The normal temperature of each grid point and day of the year were calculated from a linear regression of all observations within a 15-day period (Julian days) before and after the currently processed day of the year. A minimum of five observations before the day of interest and five observations after were required to calculate the regression. If this requirement was not met, which was sometimes the case in late fall and winter for North Channel, Green Bay, Grand Traverse Bay, Black Bay, and Nipigon Bay, the time range was extended accordingly. For instance, to calculate the normal temperature for Julian day number 215 (August 3), all images with Julian day numbers 200 (July 19) through 230 (August 18) were used for the linear regression analysis. Figure 1 shows an example of the course of the normal temperature calculated for gridpoint number 4000 of Lake Huron: 772 temperature observations of the AES and GLERL satellite measurements were available for this gridpoint.

2.4 COMBINING NORMAL ICE COVER AND TEMPERATURE DATA

The determination of ice cover from remotely sensed surface temperatures is ambiguous for several reasons:

- a) A remote instrument measures the average temperature in its field of view. Frequently the surface is broken ice cover. Thus the remotely sensed temperature consists of a mixed signal from the ice surface temperature, which can be considerably lower than 0°C , and the water surface temperature, at or above 0°C . The percentage of ice cover cannot be clearly defined from the temperature of the mixed signal if the ambient temperature of the ice surface is not known.

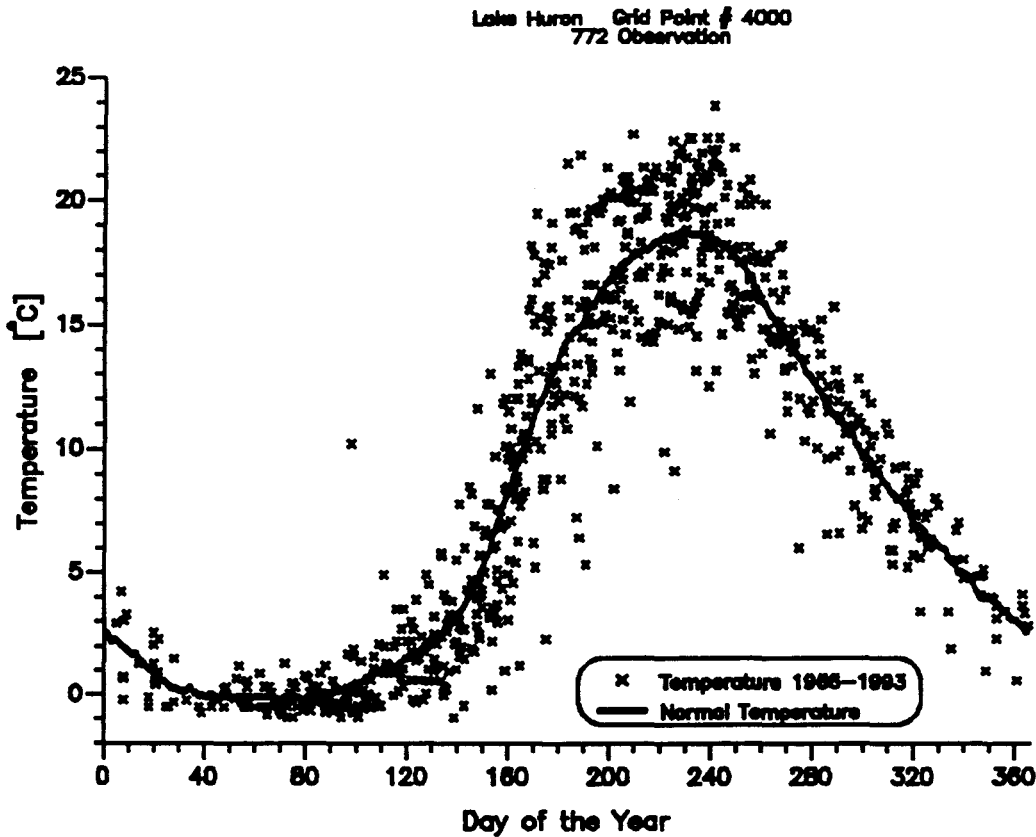


Fig. 1 Calculation of normal temperature

- b) Remote surface temperature measurements are limited to cloud-free weather: thus the frequency of usable satellite images decreases considerably in late fall and winter.
- d) The cloud-masking technique used here is optimized to reject all non-water pixels. Ice-covered pixels are therefore frequently masked as cloudy. Pixels with a temperature under -1°C are always considered cloudy.

Due to these problems, the normal ice cover documented in the *Great Lakes Ice Atlas* (Assel et al., 1983) was used to display the ice cover and ice extent of the Great Lakes.

The two data sets, normal ice cover and normal water surface temperature, are derived from different observational bases and with different techniques. Simply replacing all temperature data for each ice-covered grid point yields inconsistencies and unrealistically large temperature gradients, especially during the freezing and melting period.

Normal ice maps from the normal ice cover data base were available between 23 December and 22 April. In some lake parts, especially in shallow bay areas, parts of the lake already had considerable ice cover. To smooth the ice buildup before 23 December and the ice decay after 22 April, the ice cover data base was extended by allowing an ice buildup of 10% per day before 23 December and an equally dimensioned ice decay after 22 April. The buildup and decay rate of 10% was assumed from the ice data base.

This adjusted normal ice cover data base was merged with the normal temperature data maps. Water temperature in ice-covered areas was assumed to be 0°C. For each day with ice cover, the temperature of the normal temperature dataset was changed so that the area at or below 0°C matched the ice-covered area of the normal ice cover dataset. On the average of the ice-cover period, Lake Superior temperatures had to be decreased by 0.95°C, Lake Michigan by 1.38°C, Lake Huron by 1.06°C, Lake Erie/St.Clair by 1.48°C and Lake Ontario by 1.15°C. The positive offset of temperature versus ice cover maps is because remote temperature measurements have a good-weather bias, due to their limitation to cloud-free weather situations, and therefore tend to overestimate the normal surface temperature.

Since the locations of subzero degree pixels (ice covered) in the normal temperature dataset and ice covered grid points in the normal ice cover data base do not match in all cases, the combined ice-temperature map is smoothed using a 3x3 mean filter.

As described above, the temperatures in the normal ice cover dataset were adjusted to match those of ice-covered areas and subzero degree areas. This leads to unrealistically large temperature changes between the last ice-free day and the first ice day, and between the last day with ice cover and the first ice-free day. Before the first ice day and after the last ice day, temperature offset values were applied to the normal temperature maps to smoothly build up and decay the temperature adjustment necessary for the first and the last ice day, respectively, using a rate of 0.2°C per day.

2.5 VERTICAL TEMPERATURE PROFILES

Surface temperature is closely linked to the temperature of the underlying water column. Temperature patterns and the structure of the surface temperature field depend to some extent on the temperature gradient near the surface. Vertical mixing in the presence of a strong temperature gradient near the surface will change the surface temperature, whereas vertical mixing of a homogeneous epilimnion does not change the surface temperature. Thus, the strongest horizontal temperature gradients can be expected during the warmup period, when the shallow inshore regions have already built a stable stratification, whereas the deep lake parts are still at or close to 4°C. Small-scale temperature patches can be observed when a weak stratification has been established. A horizontally inhomogeneous wind field mixes waters of different depth and temperature, resulting in small-scale temperature patterns. The presence of a deep, homogeneous, upper water zone promotes the development of homogeneous temperature fields (Schneider, 1992).

Horizontal patterns of the surface temperature persist to some extent into the water body. The thermal structure of a lake is three dimensional. It cannot be measured directly because temperature profile measurements are rare and limited to specific measuring sites. In rare cases, well-equipped small lakes offer the possibility of interpolating the three-dimensional thermal structure of a lake from a network of profile measurements. This is rarely the case for any of the Great Lakes.

The patterns of lake surface temperature and ice cover depend mainly on energy fluxes at the water surface, heat storage, and lake dynamics. The latter process includes horizontal and vertical mixing. The depth of vertical mixing, along with the heat stored in a lake, can be displayed with vertical temperature profiles. Although the three-dimensional temperature structure cannot be shown here, the normal daily temperature profiles are very important to understand the lake surface temperature and its patterns.

Lakewide mean daily temperature profiles have been calculated using GLERL's thermodynamic and heat storage model (Croley, 1989; 1992). These temperature profiles were designed to describe the mean lakewide heat storage in the lakes.

6 BATHYMETRY DATA

For each grid point, a bathymetry value was extracted from a bathymetry data base published by Schwab and others (1980). The depth value of the nearest data point reported in the data base was assigned to each grid point. Bathymetry data are stored in 1-m depth intervals. Both mean and maximum depths, displayed in the animation program, are calculated by using extrapolated gridded data. Because of the extrapolation method of the bathymetry data and the land-water mask used, shallow inshore areas are under represented. This leads to higher average depth values than reported elsewhere.

3.0 THE COMPUTER ANIMATION PROGRAM

To display and analyze the normal temperature and ice cover data base, a computer program was developed for an IBM compatible PC with a color VGA graphics adapter. The program and data bases require 533Kb accessible RAM, a mouse, and 14.5 MB hard disk space. To execute the program Microsoft Fortran or Microsoft windows font files are required. Detailed instructions to install and use the program are given in Schneider et.al., 1993.

The program is interactive and menu driven. The main menu lets the user choose among five submenus: a) 2-D Animation, b) Horizontal Profile, c) Vertical Profile, d) Variable vs. Bathymetry, and e) Documentation. After selecting a submenu the user selects the lake(s) to be displayed. You can choose to display Lake Ontario, Lake Erie (with Lake St. Clair), Lake Huron (with Georgian Bay and North Channel), Lake Michigan and Lake Superior. Direct comparisons of different lakes are possible with submenus c) and d) by displaying several lakes simultaneously. All submenus provide a button bar to easily manipulate the animation and display and analyze different aspects of the data bases in detail. Display options can be selected by moving the cursor to the appropriate button and clicking the left mouse button, or by hitting the key displayed on the button.

The 2-D animation displays and allows manipulation of sequences of two-dimensional color coded maps of normal temperature and ice cover. The horizontal temperature profile animation allows the user to define a transect across any of the Great Lakes and display surface temperature along this transect as a line graph. The temperature and its geographical coordinates for any given point on the line graph can be displayed by pointing to it with the cursor. The vertical profile menu displays animated sequences of the modelled normal lakewide vertical temperature profiles. This data base allows the user to analyze the relationship of horizontal temperature and ice cover pattern with the heat storage in the lake. Surface temperature and ice cover depend on the energy stored in the underlying water column. The energy storage capability at a given location is directly proportional to the depth. The submenu "Variable vs. Bathymetry" lets the user investigate the dependency of surface temperature and ice cover on the depth of the lake. This module calculates the mean temperature and ice cover for each 1-m depth step and displays graphs of temperature and ice cover versus bathymetry. The graphs can be smoothed by selecting one of three smoothing algorithms. The program allows direct comparisons of different lakes by displaying multiple lakes simultaneously. The submenu documentation provides online documentation of the data base, data processing and analysis and program usage.

4.0 DISCUSSION

A normal temperature and ice cover data base for the Great Lakes of North America was produced from remote sensing data. To display and analyze the data, a computer program for IBM-compatible PCs was developed.

Temperature and ice cover patterns were developed from long-term observations and are designed to describe the normal temperature and ice cover of the Great Lakes. Since actual temperature and ice cover patterns for a specific day are determined by the current meteorological and limnological situation, they are likely to be different from the normal patterns. Interpretations of the normal patterns for a specific location and time must

be very cautious, and could yield large errors.

The normal temperature and ice cover are derived with different observational bases and different methods. Thus, merging them into one data base resulted at some locations and in some cases in discrepancies between surface temperature and ice cover.

The surface temperature measurements are based solely on remote sensing data. This technique is limited to cloud-free weather. Thus the normal surface temperature patterns are biased toward good weather. Although, under cloud-free skies, the surface temperature at night is usually lower due to increased longwave radiation, this effect is not likely to compensate for the warmer surface temperature during the day. The temperature decrease at night is limited by the fact that large energy losses at the surface lead to increasing convection. A larger water body participates in the cooling process, then in the heating, thus limiting the temperature decrease at the water surface at night. The heating of the water leads (especially under calm wind conditions) to a strongly stratified upper water zone, where most of the incoming solar radiation is absorbed. The stronger the shortwave radiation and the smaller the vertical mixing, the higher the surface temperature.

Another problem with the measuring technique of the surface temperature is that cloud-free conditions are frequently associated with specific wind situations. The likelihood of cloud-free skies is higher with north-westerly winds, than with southern and southeasterly winds, which often bring humid air to the Great Lakes region. This wind bias probably has an effect on the temperature patterns. However, since westerly winds prevail in the Great Lakes region, and since this wind direction often allows remote surface temperature measurements, the effect of wind bias on the temperature patterns is most likely small.

A comparison of the temperature patterns discussed in the *Great Lakes Surface Water Temperature Climatology* (Irbe, 1992) with the patterns shown here reveals their similarity, though both data bases were derived from different observational base. This indicates that the major surface temperature patterns are quite stable.

5.0 DATA AVAILABILITY

The normal temperature and ice cover data base and the animation program for IBM-compatible PCs are available on diskettes.

Inquiries should be addressed to:

Publications Services
NOAA/GLERL
2205 Commonwealth Blvd
Ann Arbor, MI 48105-1593
U.S.A.

or

Dr. K. Schneider
Institut für Geographie
Luisenstr. 37
80333 München
Germany

6.0 ACKNOWLEDGEMENTS

This work was completed while K. Schneider held a postdoctoral research fellowship of the National Research Council (NRC) and the Cooperative Institute of Limnological and Ecosystems Research (CILER) at NOAA/GLERL in Ann Arbor, MI. Gridded remote sensing surface temperature data acquired by the Canadian AES were provided by G. Irbe. Surface temperature images were available through NOAA's Coastal Ocean Program. Special thanks go to D.J. Schwab, G.A. Leshkevich, and G.C. Muhr (GLERL) for the support with CoastWatch products. The technical support of Mr. T. Hunter (GLERL) is greatly appreciated. Two C-subroutines to manipulate mouse movements and key strokes were written by W. Mauser of the University of Munich, Germany. The animation program was written in Microsoft FORTRAN Version 5.1.

7.0 REFERENCES

- Assel R.A., *A Computerized Ice Concentration Data Base for the Great Lakes*, NOAA Data Report ERL GLERL-24, Ann Arbor, MI, 20 pp, 1983.
- Assel R.A. and J.M. Ratkos, *A Computer Tutorial and Animation of the Normal Ice Cycle of the Laurentian Great Lakes of North America for 1960-1979*, NOAA TM ERL GLERL-76. NOAA Great Lakes Environmental Research Laboratory, Ann Arbor, MI 48105-1593, 1991.
- Assel R.A., F.H. Quinn, G.A. Leshkevich, and S.J. Bolsenga, *NOAA Great Lakes Ice Atlas*, NOAA/ GLERL, 2205 Commonwealth, Ann Arbor, MI 48105-1593, 115 pp, 1983.
- Bernstein R.L., "Sea surface temperature estimation using the NOAA 6 satellite advanced very high resolution radiometer," *Journal of Geophysical Research*, Vol. 87, pp. 9455-9465, 1982.
- Byrnes A.E., and J.R. Schott, "Correction of thermal imagery for atmospheric effects using aircraft measurements and atmospheric modelling techniques", *Applied Optics*, Vol. 25, No.15, pp. 2563-2570, 1986
- Croley T.E., II, "Verifiable evaporation modeling on the Laurentian Great Lakes", *Water Resources Research*, Vol. 25, No. 5, pp. 781-792, 1989.
- Croley T.E., II, "Long-term heat storage in the Great Lakes", *Water Resources Research*, Vol.28, No.1, pp. 69-81, 1992:
- Ewing G.C.; and E.D. McAlister, "On the thermal boundary layer of the ocean", *Science*, Vol. 131, pp. 1374-1376., 1960.
- Grassl H., "The dependence of the measured cool skin of the ocean on wind stress and total heat flux", *Boundary-Layer Meteorology*, Vol. 10, pp. 465-474, 1976.
- Irbe G.J, *Great Lakes Surface Water Temperature Climatology*, Atmospheric Environment Service, Canada, Climatological Studies No 43, 215 pp, 1992.
- Leshkevich G.A., *Lake Superior Ice Cycle - 1979*. Master's Thesis, Univ. of Michigan, 75 pp, 1982.
- Leshkevich G.A., D.J. Schwab, and G.C. Muhr, "Satellite environmental monitoring of the Great Lakes: A review of NOAA's Great Lakes CoastWatch Program", *Photogrammetric Engineering and Remote Sensing*, Vol. 59, No. 3, pp. 371-379, 1993.
- Maturi E.M., and K.G. Taggart, *Great Lakes CoastWatch Users Guide*, NOAA/NESDIS Office of Research and Applications. Washington, DC, 1993.
- McAlister E.D., and W. McLeish, "Heat transfer in the top millimeter of the ocean", *Journal of Geophysical Research*, Vol.74, No. 13, pp. 3408-3414, 1969.
- McClain E.P., W.G. Pichel, and C.C. Walton, "Comparative performance of AVHRR based multichannel sea surface temperatures", *Journal of Geophysical Research*, Vol. 90, No. C6, pp.11587-11601, 1985,

Paulson C.A., and T.W. Parker, "Cooling of a water surface by evaporation, radiation and heat transfer", *Journal of Geophysical Research*, Vol. 77, No.3, pp. 491-495, 1972.

Saunders R.W., "An automated scheme for the removal of cloud contamination from AVHRR radiances over Western Europe", *International Journal of Remote Sensing*, Vol.7, pp. 867-886, 1986.

Schneider K., *Energiefluß- und Temperaturbestimmung von Seen mit Satellitenbildern am Beispiel des Bodensees*. Seekreis Verlag Konstanz (FRG), 265 pp., 1992.

Schneider K., W. Mauser, and B. Grunwald, "The determination of energy fluxes at the water surface of Lake Constance using remotely sensed data", *Verh. Internat. Verein. Limnol.*, Vol. 24, pp.73-79, 1990.

Schneider K., and Mauser W., "The impact of the meteorological situation upon satellite derived surface skin temperature". In *Proc. 11th EARSeI Symposium*, 3-5 July 1991, Graz/Austria, pp. 270-283, 1991.

Schneider K., R.A. Assel and T.E. Croley II, *Normal Temperature and Ice Cover of the Great Lakes, A Computer Animation, Data base, and Analysis Tool*, NOAA Technical Memorandum GLERL-81, Ann Arbor, MI, 47 pp, 1993.

Schwab D.J., and D.L. Sellers, *Computerized Bathymetry and Shorelines of the Great Lakes*. NOAA Data Report ERL GLERL-16, NOAA/GLERL, Ann Arbor, MI, 13 pp., 1980.

Viehoff T., "Bestimmung der Meeresoberflächentemperature mittels hochauflösender Satellitenmessungen", *Berichte aus dem Institut für Meereskunde an der Christian-Albrechts-Univ. Kiel*, Nr.115, 119 pp., 1983.

Walton C.C. "Nonlinear multichannel algorithms for estimation of sea surface temperature with AVHRR satellite data", *Journal of Applied Meteorology*, Vol. 27, No. 2, pp.115-124., 1988.

Wilson, S.B., and J.M. Anderson, "The applicability of LOWTRAN 5 computer code to aerial thermographic data correction", *International Journal of Remote Sensing*, Vol.7, pp. 379-388, 1986.